Journal of Power Sources 399 (2018) 125–132

Contents lists available at ScienceDirect

Journal of Power Sources

journal homepage: www.elsevier.com/locate/jpowsour

Improved safety and mechanical characterizations of thick lithium-ion battery electrodes structured with porous metal current collectors

Daniel J. Noelle[a,*], Meng Wang[b], Yu Qiao[a,b]

[a] Program of Materials Science and Engineering, University of California – San Diego, La Jolla, CA, 92093, USA
[b] Department of Structural Engineering, University of California – San Diego, La Jolla, CA, 92093, USA

HIGHLIGHTS

- Porous metals current collectors enable thick electrodes with high aerial capacity.
- Interpenetrating phase composite electrodes show very safe short circuit responses.
- Optimizing electrode thicknesses with device-centric design minimizes inherent risk.
- Increased thickness composite electrode structures impart greater bending stiffness.
- Mechanically-robust electrodes support next-generation structural battery designs.

ARTICLE INFO

Keywords:
Porous metal
Foam
Current collector
Interpenetrating phase
Composite electrode
Short circuit

ABSTRACT

Porous metal current collectors enable the fabrication of thick electrode structures with improved safety margins and unique mechanical properties. Interpenetrating phase composite $LiCoO_2$ cathodes and graphite anodes with large active material loadings are formed using advanced slurry processing techniques with a submersible ultrasonic horn. Full cells with 600 μm thick electrodes demonstrate high aerial capacity of 16.7 $mAh.cm^{-2}$, improving energy density by 22% with respect to volume versus reference cells using traditional laminate composite electrode stacks. External shorting and nail penetration testing show notably suppressed joule heating currents, limiting peak temperature accrued to just 25% of the reference. Shear testing and three-point bending of individual electrodes and stack assemblies elucidate the greater role of the binder phase in the mechanical response, and that extensive characteristics such as thickness can be more influential than the intensive properties of the materials. Optimization of electrode thicknesses to balance rate capability with abuse safety is discussed, and opportunities for multifunctional application as load-bearing structural components are considered. Improved battery safety characteristics are demonstrated by reorienting the inherent components of the cell, without altering the chemical make-up, emphasizing the profound influence of structural design.

1. Introduction

Structural lithium-ion battery (LIB) designs present opportunities to increase the energy density of LIB-powered devices by undertaking both electrochemical and mechanical load-bearing functions, without modifying the underlying LIB chemistry [1]. By using energy-storing LIBs to give a device its structural form, overall mass and volume can be reduced to improve performance if the LIBs can sustainably fulfill both tasks [2,3]. Multifunctional design could aid in lightweighting of electric vehicles to extend driving range capabilities or reduce the size of personal electronics to make them easier to carry [4–6]. However, structural applications make LIBs more susceptible to physical damage, which could induce dangerous short circuit events leading to thermal runaway. As such, multifunctional LIBs with greater degrees of device integration demand more robust mechanical properties and greater margins of safety against abuse [7].

Porous metal current collectors (also referred to as metal foam current collectors) can serve as electrically-conductive structural reinforcements to enable thick electrode orientations with high aerial capacity [8–11]. When filled with an electroactive matrix of energy-storing active materials, conductive additives, and adhesive polymer binders, interpenetrating phase composite (IPC) electrode structures with unique mechanical characteristics are formed [12,13]. Unlike traditional laminate composite (LC) electrodes using 2D metal foil

* Corresponding author. 9500 Gilman Drive, MC 0085, University of California - San Diego, La Jolla, CA, 92093, USA.
E-mail address: dnoelle@eng.ucsd.edu (D.J. Noelle).

https://doi.org/10.1016/j.jpowsour.2018.07.076
Received 10 March 2018; Received in revised form 29 June 2018; Accepted 18 July 2018
0378-7753/

current collector substrates, which are coated with electroactive matrix layers on each side typically with thicknesses on the scale of 50–100 μm [8], porous metal current collectors offer a 3D foundation. In an IPC orientation, active materials can be retained close to the nearest porous metal current collector surface even when the overall electrode thickness is much larger, ensuring electron conduction uniformity and achieving high aerial loading of the electroactive matrix [9]. High capacity IPC electrodes allow for fewer bilayers to be used in cell construction compared to traditional LC electrodes, reducing the need for nonelectrochemical support components such as separators, which helps increase the volumetric energy density [14,15].

Current collectors have a significant role in short circuit discharge electrical kinetics and the electroactive matrix layer thicknesses have a notable influence on ion transport dynamics [16,17]. Upon physical damage of traditional LC electrode multilayer assemblies, direct contact between the metal foil current collectors is often the major cause of thermal runaway [18]. Electrons will rapidly discharge across low-resistance pathways afforded by the electrically-conductive metals, moving in tandem with lithium-ions travelling short distances through the electrolyte within the thin, porous electroactive matrix layers. As the electrons and the ions recombine in the cathode's active material particles, liberated joule heat can cause temperature to accrue to dangerous levels in a matter of seconds [19]. The metal foil current collectors dictate the ultimate strength of the LC electrodes, and strategic weakening of the metal foil has been shown to greatly improve safety in impact testing [20]. Thus, restructuring of the electrodes with porous metal current collectors into IPCs without strong homogeneous metal layers, as well as longer ion transport lengths, may exhibit improved safety characteristics.

The mechanical properties of the IPC electrodes are categorically different from traditional LC electrodes. In LC electrodes, the high tensile modulus metal foil component is thin, and located at the center of the structure where it imparts only low flexural stiffness to the electrode structure [21]. The porous metal current collector in heterogeneous IPC orientation reinforces the electroactive matrix throughout the thickness [12,13]. Additionally, flexural stiffness tends to increase with larger thickness components. High flexural stiffness is critical to minimizing deflection to maintain form and function when subject to mechanical loading. With these mechanical performance and safety design considerations, IPC electrodes with porous metal current collectors are investigated.

2. Experimental

2.1. Electrode processing

Porous metal current collectors were generously provided by Sumitomo Electric Industries, Ltd. The cathode's aluminum foam current collector (Al Celmet) had an initial thickness of 1.0 mm, porosity of ~95%, and pore density of ~45 PPI. The anode's copper foam current collector (Cu Celmet) had an initial thickness of 1.0 mm, porosity of ~94%, and pore density of ~105 PPI. They were filled with high-density LIB electrode slurries by hand using a spatula, and then dried under vacuum at 80 °C for 24 h. Once dry, the IPC electrodes were calendered to 600 μm thicknesses using a generic rolling press containing 2 rollers with 7.62 cm diameter in a single passthrough motion. The electrodes were cut into 1.98 cm^2 circular discs, which were subsequently characterized using a Fischer Scientific mass balance.

The high-density LIB electrode slurries, containing active materials, conductive additives, and adhesive binders, were prepared by dispersion and homogenization in processing solvents using a QSonica Q55 Sonicator with 3.2 mm diameter submersible ultrasonic horn in 10 mL Pyrex beakers (25 mm diameter, 33 mm height). Systematically applied ultrasonic power at a frequency of 20 kHz was controlled, such that standing wave resonance was maintained throughout the mixing processes. The ultrasonic friction and processing solvent cavitation was used to heat the slurry while mixing, and active stirring by hand with the horn tip ensured temperature uniformity during the homogenization process and upon cooling, as monitored by 2 type-K gage-40 thermocouples affixed to opposite sides of the beaker, connected to a Digi Sense 20250-02 Temperature Logger. The processes yielded slurries with appropriate casting viscosities at room temperature. Details of optimized power application, slurry temperature, and mixing event progression during the processes are given in section 3.1.

For cathode, $LiCoO_2$ (LCO, Lectro Plus 100, FMC Lithium), carbon black (CB, C-Energy Super C45, TIMCAL), and polyvinylidene fluoride (PVDF, MW ~534,000 powder, Sigma Aldrich) were dispersed in the ratio of LCO:CB:PVDF 93:3:4 w:w:w totaling 10.8 g into 3.6 g of N-methyl-2-pyrrolidone (NMP, anhydrous 99.5%, Sigma Aldrich). LCO, CB, and PVDF powders were premixed using a mortar and pestle prior to dispersion in NMP.

For anode, graphite (TIMREX SLP30, TIMCAL), CB, carboxymethylcellulose sodium salt (CMC, medium viscosity, Sigma Aldrich), and styrene-butadiene rubber (SBR, MTI Corporation) were dispersed in the ratio of graphite:CB:CMC:SBR 93:2:2:3 w:w:w:w totaling 3.15 g into 3.5 g of deionized water (DI). The CMC salt was first dissolved in DI water. The SBR liquid was subsequently mixed in solution at 80 °C for 1 h using a Corning PC-420D Stirring Hot Plate. Then, graphite and CB powders were fully mixed into the solution using a glass stir bar prior to ultrasonic agitation. Graphite and CB powders were premixed using a mortar and pestle before being added to the DI/CMC/SBR solution.

2.2. Electrochemical performance and abuse characterization

LIR2032 format full cells were constructed for electrochemical characterization and short circuit abuse testing of the IPC electrode assemblies. The electrode stacks were assembled in uniaxial orientation using one cathode disc, one anode disc, one trilayer separator layer (Celgard 2320), and a copper foam spacer used to secure electrical and thermal contact with the cell case. The electrodes and separators were submerged in 1 M $LiPF_6$ EC:EMC 1:1 w:w electrolyte (BASF Selectilyte LP50), and subjected to reduced pressure atmosphere of 85 mmHg at room temperature for 3 min, ensuring complete wetting prior to cell construction. Cells were sealed using an MTI Corporation MSK-100 hydraulic press with CR20XX crimping die set inside an MBraun LABStar glovebox with water-free argon atmosphere (H_2O < 0.5 ppm).

Galvanostatic analysis was carried out using a Neware BTS4000-5V10 mA Battery Analyzer. Cycling was performed at 0.38 mA cm^{-2} constant current rate between 3.0 V and 4.2 V, which took ~45 h after the initial two conditioning cycles for each charging step and discharging step, denoted here as the C/45 current rate for this IPC cell system. Discharging rate capabilities at constant currents of 0.75 mA cm^{-2}, 1.12 mA cm^{-2}, 1.50 mA cm^{-2}, and 1.88 mA cm^{-2} following 0.38 mA cm^{-2} constant current charging steps were also evaluated.

The mass and dimensions of galvanostatic-conditioned electrode stack assemblies and components were measured in the discharged state with a Fischer Scientific mass balance and displacement micrometer inside the glovebox. Measurements were made immediately upon deconstruction using the MTI Corporation MSK-100 hydraulic press with CR20XX disassembling die set. These measurements were taken to evaluate energy density accounting for electroactive matrices, current collectors, separator, and saturated electrolyte mass internal to the stack, while excluding mass and volume contributions from cell cases, connecting tabs/spacers, and electrolyte external to the stack.

The LIB cells were subjected to external shorting and nail penetration testing, performed using the same testing procedures described in Ref. [16]. In external shorting, current response was directly measured using a Neware BTS3000-5V6A Battery Analyzer upon discharge with a 110 mΩ resistor. Nail penetration was performed using a 2.7 mm diameter, 38 mm long 304 stainless steel nail. In both experiments cell temperature response was documented using type-K gage-40 thermocouple affixed to the cell case by polyimide tape. Cells used in abuse

testing were preconditioned by cycling twice at C/45 between 3.0 V and 4.2 V, charged to 33.1 mAh capacity, and then given a 24 h resting period prior to short circuit initiation.

Electrochemical performance and abuse characterizations were compared against commercially-produced LIR2032 format LCO/graphite 40 mAh cells with traditional LC electrode stack assemblies, purchased from AA Portable Power Corporation. They were subjected to identical electrochemical conditioning, abuse testing, and mass/dimension measurement protocols as the cells assembled with IPC electrodes.

2.3. Mechanical property characterization

Measurements of force and displacement were made to elucidate the roles of current collector reinforcements, electroactive matrix layers, and multilayer electrode assembly orientations using an Instron 5582 Testing Machine. Aluminum and copper foil current collectors as well as LCO and graphite LC electrodes were purchased from MTI Corporation for comparison with the porous metal current collectors and the IPC electrode units.

Shear testing was performed on individual current collector and electrode layers using a custom-made load cell that slowly compressed the center of 1.98 cm^2 circular samples with a 3.2 mm diameter piston into a 3.8 mm diameter gap at a rate of 10 $\mu m\, s^{-1}$, until fracture occurred. Three-point bending was performed on individual electrode layers, as well as multilayer stacks with separator interfaces, all precut to widths of 12.5 mm and loaded at a rate of 10 $\mu m\, s^{-1}$ across the center of a 12.5 mm support span. Multilayer assemblies were compared on 2.5 mm thickness basis. The assemblies were formed with cathode/separator/anode/separator alternating bilayers vacuum-sealed in polypropylene bags to secure interlayer contact. The intended testing thickness was produced with 8 and 2 electrode bilayer assemblies for LC and IPC electrodes, respectively.

3. Results and discussion

3.1. Electrode fabrication and electrochemical performance

The metal foam current collectors are impregnated with slurries exhibiting high active material loading densities to produce the IPC electrodes. The slurries have LCO and graphite loadings of ~1.5 $g\, mL^{-1}$ and ~0.7 $g\, mL^{-1}$, enabling realization of high aerial capacity electrodes with active material loadings of 138 $mg\, cm^{-2}$ and 55 $mg\, cm^{-2}$ after drying and calendering for cathode and anode, respectively. The optimized slurry processing mixing procedure, ultrasonic power application sequence, and processing temperature results for 3.5 mL processing solvent bases are depicted in Fig. 1.

The realized active material loadings equate to theoretical reversible current capacities of 19.2 $mAh.cm^{-2}$ (140 $mAh.g_{LCO}{}^{-1}$) for the LCO electrodes up to 4.2 V vs. Li^+/Li and 20.5 $mAh.cm^{-2}$ (372 $mAh.g_{graphite}{}^{-1}$) for the graphite electrodes down to 0.01 V vs. Li^+/Li. However, such high aerial current capacities were determined to be unsuitable for lithium metal counter electrodes to be used in examining the individual IPC electrode capacities experimentally in half cell formation. Excessive electrolyte decomposition supporting continuous lithium metal surface passivation upon rampant dendrite growth produced high impedance lithiation characteristics and consistently occurring internal short circuit failure during the initial two conditioning cycles, without producing reliable information about the capabilities of the working electrodes of interest. As such, half cell testing experiments are not considering to be of value to this investigation.

The IPC electrode full cells with LCO cathode and graphite anode achieve a reversible capacity of 16.7 $mAh.cm^{-2}$ following three formation cycles when charged and discharged at 0.38 $mA\, cm^{-2}$, approaching 99.4% columbic efficiency after 10 cycles (~900 h of testing). This full cell capacity equates to 121 $mAh.g_{LCO}{}^{-1}$, indicating suitable usage of the large active material loading, after irreversible capacity loss to solid electrolyte interface formation on the graphite electrode is considered. At higher discharge rates, the cells exhibit diminished discharge capacity capabilities. Reported in Fig. 2, these performance characteristics are consistent with other investigations on thick IPC electrodes with porous metal current collectors [8,9], but respectable gains in aerial and volumetric electrode capacities are demonstrated, as facilitated by advanced slurry processing procedures.

Commercially-produced LIR2032 units with LC electrodes of the same LCO/graphite chemistry exhibit better rate performance at room temperature. In terms of energy densities, the LC electrode stack assembly is 11% higher with respect to mass, while the IPC electrode stack assembly is 22% higher with respect to volume, as noted in Table 1.

3.2. External short circuit and nail penetration

As postulated, thick IPC electrodes supported by porous metal current collectors are considerably safer than traditional LC units with metal foil current collectors. Upon external shorting, the electrically-controlled capacitive discharge current measured for the modified IPC cells is only 38% of the reference LC cells in the first 3 s after initiation. Due to the increased thickness, the continued ionically-controlled, sustained discharge current averages only 14% of the reference values over the following 5 min. These joule heating dynamics limit the maximum peak temperature increase to just 25% of the reference external shorting experiments, with consistent results observed in nail penetration testing. For fair comparison, both traditional LC electrode and modified IPC electrode units are charged to the current capacity of 33.1 mAh. Short circuit current dynamics and cell temperature responses are shown alongside images of the electrodes in Fig. 3.

3.3. Balancing rate capability and short circuit safety

The safety characteristics of LIB cells are closely coupled to their discharge rate capabilities. Prior to discharge initiation, the concentration of lithium-ions in electrolyte is uniform across the characteristic length of the cell. When discharge begins, ions in the electrolyte of the cathode region are uptaken by the LCO active material particles, while simultaneously, ions are liberated from the graphite active material particles into the electrolyte of the anode region. In this manner, a concentration imbalance forms a chemical potential gradient which drives mass transfer of lithium-ions through the electrolyte across the separator membrane from the anode region to the cathode region. The rate these ions are capable of moving is dictated by their diffusivity in the organic electrolyte where they are located. The pathlength charge-carrying lithium-ions need to travel in electrolyte to balance the concentration difference primarily depends on the orientation of the electrodes.

When the discharge current is fast enough to remove ions from the electrolyte of the cathode region more quickly than they are replenished by ions crossing the separator interface from the anode region, electrolyte polarization impedance manifests. Under excessive constant current discharge control, the consequent overpotential bias causes the lower operating range 3.0 V cutoff to be realized with reduced current capacity discharged, defining the cells' sustained rate capabilities in many cases. If a low resistance short circuit discharge pathway is formed, the reservoir of charge-transferable lithium-ions in the electrolyte of the cathode region is rapidly depleted in a brief capacitive joule heating event. The short circuit current is subsequently throttled to lower rates dependent on the ions' abilities to traverse the separator interface from the anode region to recombine with electrons in the LCO active material particles [16].

The electrode thickness has a significant role in both rate capability and short circuit response. It is standard practice to use LC electrodes

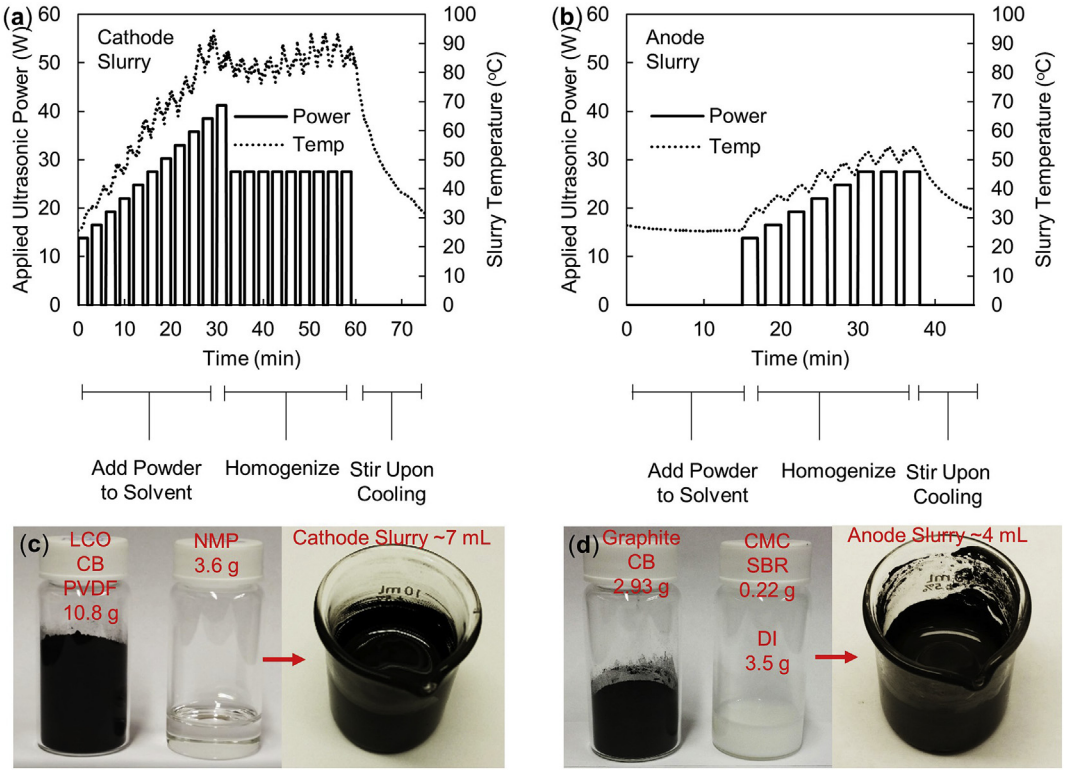

Fig. 1. Ultrasonic power application, mixing sequence, and consequent temperature dynamics of (**a**) cathode and (**b**) anode slurries processed using QSonica Q55 Sonicator with 3.2 mm diameter submersible ultrasonic horn homogenized in 10 mL Pyrex beakers. (**c**) Images of the $LiCoO_2$ (LCO), carbon black (CB), and polyvinylidene fluoride (PVDF) materials dispersed in N-methyl-2-pyrrolidone (NMP) to produce finished high-density cathode slurry. (**d**) Images of graphite, CB, carboxymethyl cellulose (CMC), and styrene-butadiene rubber (SBR) dispersed in deionized water (DI) to produce finished high-density anode slurry.

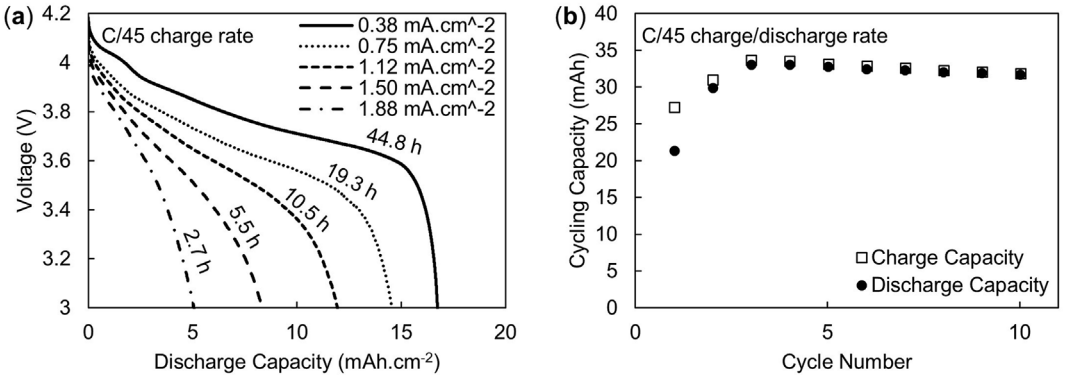

Fig. 2. (**a**) Voltage/capacity profiles and times for increasing discharge current rates and (**b**) formation/cycling capacity for 600 μm thick, 1.98 cm^2 interpenetrating phase composite $LiCoO_2$/graphite electrodes arranged in uniaxial full cell orientation in LIR2032 format coin cells.

with thinner electroactive matrix layers to minimize the pathlength that ions would need to travel to retain low polarization impedances, thus increasing sustained rate capabilities. This characteristic is common in power cells, but reduces energy-storing active material mass relative to the contributions of the current collector reinforcements, sacrificing energy density [8]. The thick IPC electrodes examined here take the opposite approach, increasing the pathlength for the purpose of exacerbating polarization impedances in a short circuit event to curb sustained joule heating rate responses.

Electrodes need to be thin enough to realize the rate capabilities required for optimal performance of the devices they are intended to power, but no thinner. Rate capabilities in excess of what is needed incur unnecessary added risk without further benefit. Porous metal current collectors allow for versatility in designing LIB cells with fast rate capabilities, long run-times, and balanced intermediates. IPC electrodes have shown they can retain full use of all active materials loaded at thicknesses as little as 100 μm and as high as 1200 μm [8,15]. Using thin IPC electrodes with high current collector pore densities has been shown to improve rate capabilities for $LiFePO_4$ electrodes by enhancing electron conduction [14], which is useful for devices like heavy-duty power tools. Using thick, robust IPC electrodes to continuously supply low power over long run-times could greatly improve safety margins in applications where they are of the utmost importance, as is demanded of advanced communication and tracking electronics carried by dismounted soldiers with 72 h mission life requirements [22]. Optimal thicknesses for devices with intermediate power requirements, like smart phones and other personal electronics, could be selected to satisfy power demands with the least risk retention.

Table 1
Electrochemical characteristics of LIR2032 cells with laminate composite (LC) electrodes and interpenetrating phase composite (IPC) electrodes.

Assembly	LIR2032 w/LC Electrodes	LIR2032 w/IPC Electrodes
Cathode		
Active Material	LCO	LCO
Binder	NMP soluble (e.g. PVDF)	PVDF
Current Collector	Aluminum foil (15 μm thick)	Aluminum foam
Electroactive Matrix Thickness	57.5 μm (each side)	600 μm
Active Material Mass	–	274 mg
Total Mass (Dry)	–	320 mg
Anode		
Active Material	Graphite	Graphite
Binder	Water soluble (e.g. CMC)	CMC:SBR 2:3 w:w
Current Collector	Copper foil (10 μm)	Copper foam
Electroactive Matrix Thickness	67.5 μm (each side)	600 μm
Active Material Mass	–	109 mg
Total Mass (Dry)	–	198 mg
Full Cell		
Production Means	Commercial Factory	Handmade
Charge/Discharge Step Time	10 h	45 h
Voltage Range	3.0 V–4.2 V	3.0 V–4.2 V
Discharge Capacity	40.0 mAh	33.1 mAh
Discharge Energy	153 mWh	124 mWh
Electrode Area	7.70 cm^2	1.98 cm^2
Electrode Orientation	Biaxial	Uniaxial
Electrode Stack Thickness	2.52 mm	1.24 mm
Electrode Stack Volume	370 μL	245 μL
Total Electrode Stack Mass	781 mg	696 mg
Volumetric Energy Density	414 W h/L	506 W h/L
Gravimetric Energy Density	196 W h/kg	178 W h/kg

3.4. Shear testing and three-point bending

The force-displacement curves show the IPC electrodes are more robust against shear loading than the LC electrodes, withstanding forces more than two times greater prior to fracture. For the IPC electrodes, complete fracture occurs upon failure such that the damaged area is electrically disconnected from the remaining electrode, while the metal foil current collectors and LC electrodes exhibit only partial breakage. Fracture responses demonstrating complete separation of the damaged area are favorable in abusive impact conditions from a safety standpoint, as discussed in a previous report [20]. In both LC and IPC electrodes, the anodes exhibit higher maximum loads and post-yield displacements than the cathodes. The mechanical response results and images after testing are shown in Fig. 4.

For both cathode and anode, the metal foil current collectors and reference LC electrodes behave largely the same, demonstrating that the electroactive matrix coated layers do not make significant contributions to the mechanical response under abusive shear, and the metal foil reinforcements carry the bulk of the mechanical load. Conversely, the porous metal current collectors experience notably larger post-yield displacements under less stress than the modified IPC electrodes, which withstand larger mechanical loads prior to fracture. This result indicates the electroactive matrix has a consequential influence on the shear response in the IPC orientation, sharing the mechanical load with the porous metal current collector reinforcements.

In three-point bending, the individual IPC electrodes demonstrate bending stiffnesses of 4.9 N mm^{-1} and 5.9 N mm^{-1} for cathode and anode respectively, an order of magnitude greater than the LC electrodes which exhibit 0.37 N mm^{-1} and 0.14 N mm^{-1}. These extensive properties persist despite the larger flexural moduli of the LC electrodes, exhibiting 6.87 GPa and 1.80 GPa for the cathode and anode, respectively, compared to just 0.83 GPa and 1.01 GPa for the IPC electrodes. The result demonstrates that electrode thickness and component orientation can have a greater influence on mechanical performance characteristics than the intensive material properties of those individual components. Furthermore, the lower flexural moduli of the IPC electrodes suggest the low-tensile-modulus electroactive matrices play greater roles in load-bearing functionality than they do in LC electrodes, which is consistent with the observations noted in shear testing. Results of the three-point bending tests are depicted in Fig. 5.

When multiple LC or IPC layers are stacked with separators and vacuum-sealed together in polymer bags, as is characteristic of practical LIB pouch cell formats, three-point bending of the electrode stack

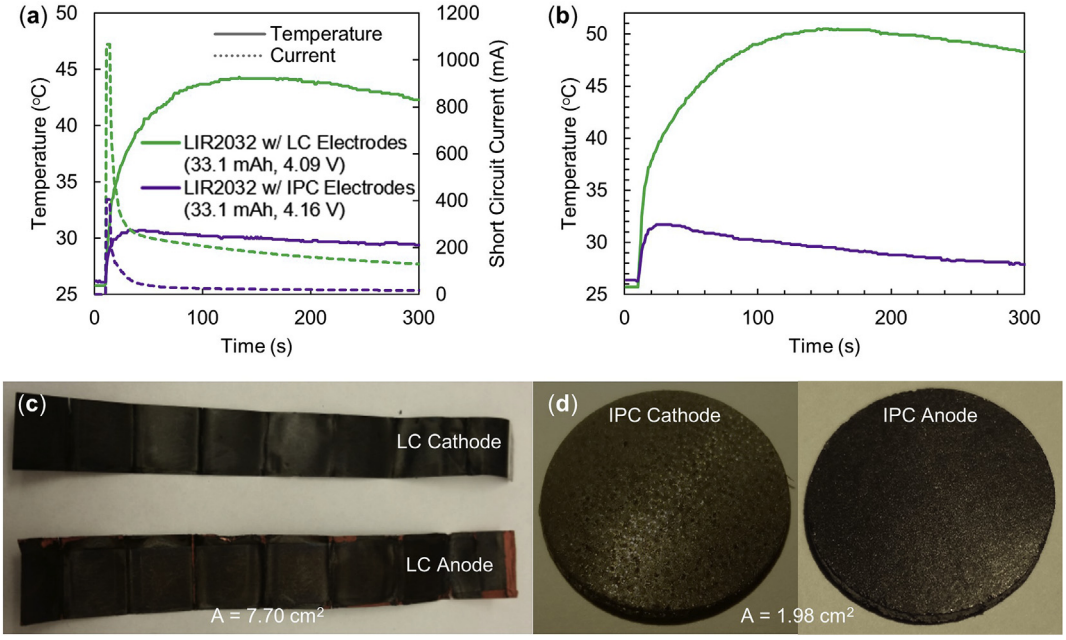

Fig. 3. (**a**) External short circuit temperature response and discharge current dynamics of LIR2032 coin cells with laminate composite (LC) electrodes and interpenetrating phase composite (IPC) electrodes. (**b**) Nail penetration temperature response. Images of (**c**) LC electrodes and (**d**) IPC electrodes used for electrochemical evaluation and abuse testing.

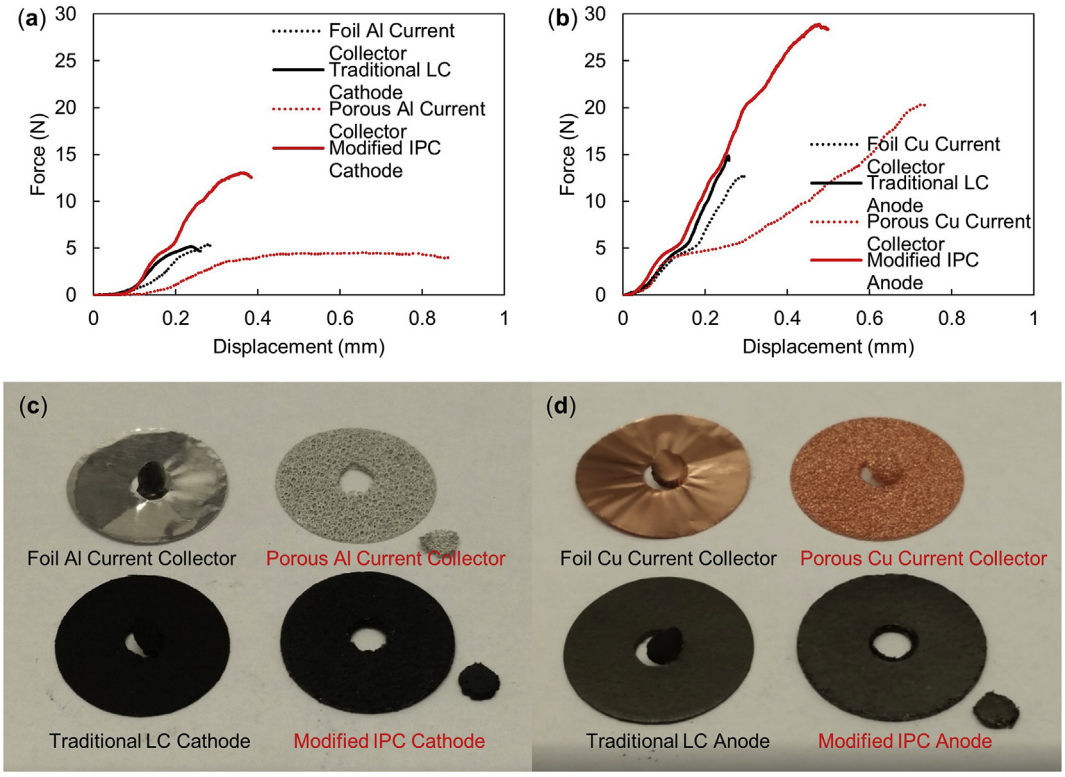

Fig. 4. Shear force-displacement profiles of current collector and electrode 1.98 cm^2 samples with a 3.2 mm diameter piston pressing the geometric centers into a 3.8 mm diameter gap at a rate of 10 $\mu m\ s^{-1}$ for (**a**) aluminum current collectors and cathodes as well as (**b**) copper current collectors and anodes in laminate composite (LC) and interpenetrating phase composite (IPC) formations. Images show fracture of (**c**) cathodes, (**d**) anodes, and current collectors after testing.

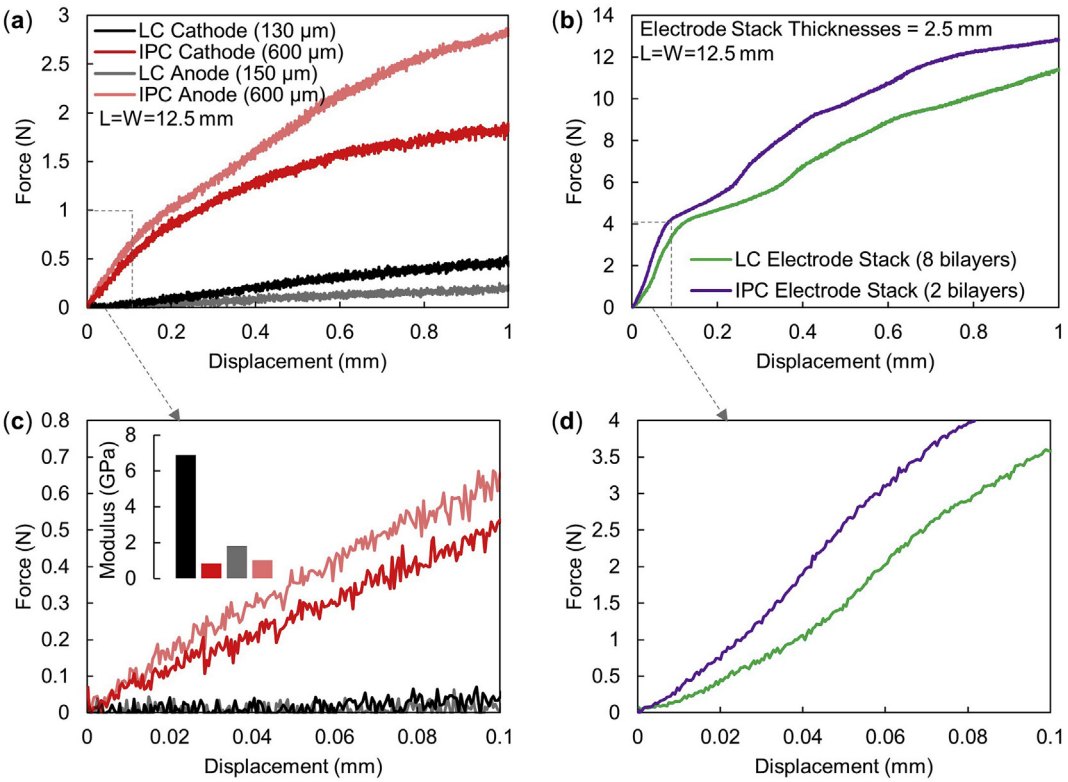

Fig. 5. (**a**) Three-point bending force-displacement profiles for individual laminate composite (LC) and interpenetrating phase composite (IPC) electrodes and (**b**) electrode stack assemblies totaling 2.5 mm thickness, all tested with 12.5 mm width and support length loaded at a rate of 10 $\mu m\ s^{-1}$. Enhanced images of regions used to determine (**c**) the flexural modulus for the individual electrodes and (**d**) bending stiffness for the multilayer assemblies.

assemblies are evaluated on equivalent 2.5 mm thickness basis. The force-displacement curves are fairly linear up to 75 μm displacement, equating 3% deflection, but not perfectly so, likely due to interlayer sliding and reorientation under stress, which is more pronounced in the LC stacks which have more layers. Electrode assemblies exhibit average bending stiffnesses of $34.2\,N\,mm^{-1}$ for the LC electrodes and $48.8\,N\,mm^{-1}$ for the IPC electrodes until a yield load of 3.5 N is reached, at which point the weaker electroactive matrix phases begin to fail under the compression. This result reaffirms that IPC electrode assemblies can be preferable to the LC electrodes when structural functions are to be considered. That said, it should be noted that in practice, mechanical properties are also influenced by cell orientation, formation techniques, state-of-charge, etc., which in turn influence electrochemical functionality and require testing and optimization under the intended operating conditions of the particular cell unit.

3.5. Prospects and challenges for multifunctional application

The IPC electrodes formed with porous metal current collectors show greater bending stiffness and volumetric energy density than units with comparable current capacity and shape constructed with LC electrodes, in addition to being significantly safer in short circuit events. These characteristics are desirable to have in devices with greater degrees of cell integration. Such improvements are profound considering the LIB components have simply been reoriented, and the chemical make-up of the cells has not been altered. Thus, similar modifications with porous metal current collectors are expected to be compatible with many modern and future LIB chemistries and cell designs that would otherwise use traditional aluminum or copper foil current collector materials in LC formations, imparting their unique traits to improving robustness in LIBs which have larger energy densities and perform higher risk functions. However, optimization of the porous metal current collector geometry and further development of the electroactive matrices is necessary to be viable for multifunctional implementation, such that the LIB cells can carry a physical load while retaining sustainable electrochemical storage functionality.

Larger pore densities and thread thicknesses of porous metals increase the bending stiffness of IPCs, but tend to have lower porosity and larger masses [13]. In this demonstration, the ~45 PPI pore density aluminum foam current collector accounts for less than 8 wt% of the lower stiffness cathode, while the ~105 PPI pore density copper foam current collector accounts for more than 38 wt% of the higher stiffness anode. Depending on the structural load the LIB is intended carry, the aluminum foam's pore density and thread thickness could be increased to impart greater bending stiffness, or the copper foam's pore density and thread thickness could be decreased to improve the gravimetric energy density, which is slightly lower than the reference LC electrode cells in this example. If thinner electrodes are used, that would notably influence the bending stiffness, and current collectors may be precut considering the intended thicknesses of the fully formed IPC electrodes in order to retain their characteristic mechanical and mass contributions to the heterogeneous electrode structures. However, even if the gravimetric energy density of the IPC cell is lower than a traditional LC cell, it could still be preferable if the overall mass contribution of the cell to the LIB-powered device is reduced because it is able to perform multiple functions by replacing redundant load-bearing components, or if reducing volume is a more important design factor [2].

For structural LIBs using IPC electrode orientations to be practical, they must perform their primary function as electrochemical storage devices dutifully when subjected to physical-loading that is not normally imposed on traditional LIB cells. Performance degradation for LIB electrodes may occur upon interfacial debonding between the binder phase and active material particles within the electroactive matrix, as well as delamination of the electroactive matrix layers from the current collector reinforcements [23], which is a common challenge in electrodes containing active materials that experience large stain due to volume expansion upon lithiation [24]. These modes of degradation are particularly concerning when considering the prospect that a LIB would be subject to continuous static loading and dynamic mechanical stress cycles in the field that could cause debonding, limiting the cyclability to be shorter than it would under unstressed conditions. Additionally, unmitigated strain the IPC electrodes are exposed to could cause the sharp edges of the porous metal current collectors to pierce the separator layers and cause a short circuit. While such events would be much less dangerous than if they were to occur in traditional LC units, they still need to be treated as a risk factor. As such, the electroactive matrix and separator layers need to be strengthened for the IPC units to be realistically considered for multifunctional implementation, and further experimentation verifying simultaneous galvanostatic cycling and mechanical loading requirements can be sustainably realized must be performed upon further development.

The mechanical tests performed in this study show that the electroactive matrix phase plays a notable role in the load-bearing response of the IPC electrode. The tensile modulus and adhesive strength of the electroactive matrices are largely imparted by the binder phases, which need to be improved to tolerate mechanical stress. The CMC binder of the anode layers has good adhesive strength and its SBR component facilitates a degree of compliance when strain is experienced. However, the PVDF binder of the cathode layers has relatively poor mechanical properties, especially upon wetting by organic carbonate-based electrolyte, and is likely to fail [24]. Additionally, thin polypropylene separators are not puncture resistant. The fact that the binder phases and separator layers of IPC units would assume undue burden in structural applications demands they would need to be replaced with more robust materials. Solid-state and gel electrolyte separator layers have received considerable research attention [25], and next generation binders developed in the pursuit of large-strain-inducing active materials and environmentally friendly electrode processing could be adapted to support structural LIB designs [24,26]. With supporting modifications, the porous metal current collectors facilitating thick electrodes showing excellent abuse tolerance are promising materials for further development of multifunctional LIBs.

4. Conclusion

Porous metal current collectors facilitate formation of thick, high aerial capacity lithium-ion battery electrodes with improved safety and unique mechanical characteristics. By reorienting the electrode materials from laminate composite into interpenetrating phase composite formations, short circuit currents and joule heating rates are significantly suppressed to prevent temperature accruement that could lead to thermal runaway in physically abusive events. Increasing thickness also imparts greater flexural bending stiffness to the electrodes which make them attractive for multifunctional battery applications, where they might assist in load-bearing structural functions to improve overall device performance and safety margins. Simultaneously, energy density is increased by reducing volumetric contributions from nonelectrochemical support components such as separators, due to the reduced geometric interfacial area. A technical challenge of this safety-first design approach comes at the expense of rate capability, which precludes its use in certain applications. Further optimization of the electrode thicknesses, component orientations and materials are discussed to satisfy the differing needs of battery-operated devices, focusing on device-centric battery design to improve safety margins and facilitate multifunctional structural implementation.

Acknowledgements

We would like to thank Sumitomo Electric Industries, Ltd. for contributing Aluminum Celmet and Copper Celmet materials for testing as current collectors and appreciate their generous support of this investigation. All data collected for analysis was obtained using

laboratory resources of the Department of Structural Engineering at the University of California – San Diego. This research did not receive any specific grant from funding agencies in the public, commercial, or not-for-profit sectors.

References

[1] P. Liu, E. Sherman, A. Jacobsen, Design and fabrication of multifunctional structural batteries, J. Power Sources 189 (2009) 646–650, https://doi.org/10.1016/j.jpowsour.2008.09.082.

[2] J.F. Snyder, E.B. Gienger, E.D. Wetzel, Performance metrics for structural composites with electrochemical multifunctionality, J. Compos. Mater. 49 (2015) 1835–1848, https://doi.org/10.1177/0021998314568167.

[3] L.E. Asp, E.S. Greenhalgh, Structural power composites, Compos. Sci. Technol. 101 (2014) 41–61, https://doi.org/10.1016/j.compscitech.2014.06.020.

[4] M. Wang, L. Zhu, A.V. Le, D.J. Noelle, Y. Shi, Y. Zhong, F. Hao, X. Chen, Y. Qiao, A multifunctional battery module design for electric vehicle, J. Mod. Transp. 25 (2017) 218–222, https://doi.org/10.1007/s40534-017-0144-8.

[5] Y. Zhang, J. Ma, A.K. Singh, L. Cao, J. Seo, C.D. Rahn, C.E. Bakis, M.A. Hickner, Multifunctional structural lithium-ion battery for electric vehicles, J. Intell. Mater. Syst. Struct. 28 (2017) 1603–1613, https://doi.org/10.1177/1045389X16679021.

[6] P. Ladpli, R. Nardari, F. Kopsaftopoulos, Y. Wang, F. Chang, Design of multifunctional structural batteries with health monitoring capabilities, 8th Eur. Work. Struct, Heal. Monit., Bilbao, Spain, 2016, pp. 5–8.

[7] F. Hao, X. Lu, Y. Qiao, X. Chen, Crashworthiness analysis of electric vehicle with energy-absorbing battery modules, J. Eng. Mater. Technol. 139 (2016) 1–4, https://doi.org/10.1115/1.4035498.

[8] J.S. Wang, P. Liu, E. Sherman, M. Verbrugge, H. Tataria, Formulation and characterization of ultra-thick electrodes for high energy lithium-ion batteries employing tailored metal foams, J. Power Sources 196 (2011) 8714–8718, https://doi.org/10.1016/j.jpowsour.2011.06.071.

[9] G.F. Yang, K.Y. Song, S.K. Joo, Ultra-thick Li-ion battery electrodes using different cell size of metal foam current collectors, RSC Adv. 5 (2015) 16702–16706, https://doi.org/10.1039/C4RA14485F.

[10] J. Nishimura, K. Okuno, K. Kimura, K. Goto, H. Sakaida, A. Hosoe, R. Yoshikawa, Development of new aluminum-celmet current collector that contributes to the improvement of various properties of energy storage devices, SEI Tech. Rev. 76 (2013) 40–44.

[11] H. Nara, T. Yokoshima, H. Mikuriya, S. Tsuda, T. Momma, T. Osaka, The potential for the creation of a high areal capacity lithium-sulfur battery using a metal foam current collector, J. Electrochem. Soc. 164 (2017) A5026–A5030, https://doi.org/10.1149/2.0381701jes.

[12] Z. Yuan, N. Rayess, N. Dukhan, Modeling of the mechanical properties of a polymer-metal foam hybrid, Procedia Mater. Sci. 4 (2014) 207–211, https://doi.org/10.1016/j.mspro.2014.07.602.

[13] N. Dukhan, N. Rayess, J. Hadley, Characterization of aluminum foam-polypropylene interpenetrating phase composites: flexural test results, Mech. Mater. 42 (2010) 134–141, https://doi.org/10.1016/j.mechmat.2009.09.010.

[14] G.F. Yang, K.Y. Song, S.K. Joo, A metal foam as a current collector for high power and high capacity lithium iron phosphate batteries, J. Mater. Chem. A. 2 (2014) 19648–19652, https://doi.org/10.1039/C4TA03890H.

[15] H. Sakaida, K. Goto, K. Kimura, K. Okuno, J. Nishimura, A. Hosoe, Aluminum-celmet—aluminum porous metal with three-dimensional consecutive pores, SEI Tech. Rev. (2017) 87–92.

[16] D.J. Noelle, M. Wang, A.V. Le, Y. Shi, Y. Qiao, Internal resistance and polarization dynamics of lithium-ion batteries upon internal shorting, Appl. Energy 212 (2018) 796–808, https://doi.org/10.1016/j.apenergy.2017.12.086.

[17] T.G. Zavalis, M. Behm, G. Lindbergh, Investigation of short-circuit scenarios in a lithium-ion battery cell, J. Electrochem. Soc. 159 (2012) A848, https://doi.org/10.1149/2.096206jes.

[18] S. Santhanagopalan, P. Ramadass, J. Zhang, Analysis of internal short-circuit in a lithium ion cell, J. Power Sources 194 (2009) 550–557, https://doi.org/10.1016/j.jpowsour.2009.05.002.

[19] R. Spotnitz, J. Franklin, Abuse behavior of high-power, lithium-ion cells, J. Power Sources 113 (2003) 81–100, https://doi.org/10.1016/S0378-7753(02)00488-3.

[20] M. Wang, A.V. Le, D.J. Noelle, Y. Shi, Y.S. Meng, Y. Qiao, Internal-short-mitigating current collector for lithium-ion battery, J. Power Sources 348 (2017) 84–93, https://doi.org/10.1016/j.jpowsour.2017.03.004.

[21] B.Y. Wyser, C. Pelletier, J. Lange, Predicting and determining the bending stiffness of thin films and laminates, Packag. Technol. Sci. 14 (2001) 97–108.

[22] T.B. Atwater, P.J. Cygan, F.C. Leung, Man portable power needs of the 21st century. I. Applications for the dismounted soldier. II. Enhanced capabilities through the use of hybrid power sources, J. Power Sources 91 (2000) 27–36, https://doi.org/10.1016/S0378-7753(00)00484-5.

[23] S. Lee, J. Yang, W. Lu, Debonding at the interface between active particles and PVDF binder in Li-ion batteries, Extrem. Mech. Lett. 6 (2016) 37–44, https://doi.org/10.1016/j.eml.2015.11.005.

[24] A. Magasinski, B. Zdyrko, I. Kovalenko, B. Hertzberg, R. Burtovyy, C.F. Huebner, T.F. Fuller, I. Luzinov, G. Yushin, Toward efficient binders for Li-Ion battery Si-Based Anodes : polyacrylic acid, Appl. Mater. Interfaces 2 (2010) 3004–3010, https://doi.org/10.1021/am100871y.

[25] J.G. Kim, B. Son, S. Mukherjee, N. Schuppert, A. Bates, O. Kwon, M.J. Choi, H.Y. Chung, S. Park, A review of lithium and non-lithium based solid state batteries, J. Power Sources 282 (2015) 299–322, https://doi.org/10.1016/j.jpowsour.2015.02.054.

[26] N. Loeffler, T. Kopel, G. Kim, S. Passerini, Polyurethane binder for aqueous processing of Li-Ion battery, J. Electrochem. Soc. 162 (2015) 2692–2698, https://doi.org/10.1149/2.0641514jes.